CRYSTAL GROWTH & DESIGN

ARTICLE

pubs.acs.org/crystal

Making Benzamide Cocrystals with Benzoic Acids: The Influence of Chemical Structure.

Published as part of a virtual special issue of selected papers presented at the 2010 Annual Conference of the British Association for Crystal Growth (BACG), Manchester, UK, September 5−7, 2010.

Colin C. Seaton*,† and Andrew Parkin‡

†School of Chemical Engineering & Analytical Science, The Mill, University of Manchester, Oxford Road, Manchester, United Kingdom, M13 9PL,

‡WestCHEM, Department of Chemistry, University of Glasgow, University Avenue, Glasgow, United Kingdom

ABSTRACT: An investigation into the creation of cocrystals of benzamide and substituted benzoic acids was undertaken and four new cocrystals were structurally characterized by single-crystal X-ray diffraction. The attempted cocrystallizations were only successful in those cases where electron-withdrawing functional groups were present as substituents on the benzoic acid. This experimental observation was supported by computational studies, which indicated that in these cases the intermolecular acid···amide interaction between the acid and benzamide was strengthened. A correlation between the interaction energy and the Hammett substitution constant in the applicable cases was displayed. The calculated energy of interaction between benzamide/salicylic acid dimers and benzamide/benzoic acid dimer are the same, yet only benzamide/salicylic acid forms a cocrystal. Lattice energy calculations on the salicylic acid/benzamide crystal structure and hypothetical benzoic acid/benzamide cocrystal structures indicate a difference of approximately 50 kJ mol^{-1} in energy between these systems, suggesting that the other crystal packing forces are not sufficient to stabilize the benzoic acid/benzamide cocrystal.

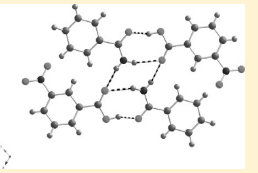

INTRODUCTION

The creation of multicomponent crystalline materials (such as salts, molecular complexes or cocrystals) is an area of expanding growth,[1] driven by the study of pharmaceutical cocrystals.[2] These materials offer a possible route for the modification of the physicochemical properties of an active pharmaceutical ingredient (API) without changing the pharmaceutical activity. However, the discovery of new complexes is currently often serendipitous and so the designed creation of such materials with required properties, still requires the development of a deeper understanding of the processes that control their formation.

The key design tool used to select suitable coformers for a given substance is the concept of a supramolecular synthon.[3] These are frequently occurring intermolecular interactions that are expected to bind the two components together within in the crystal, commonly identified through database searching. Often the supramolecular synthons are considered in isolation from the rest of the molecule; however interactions between the other functional groups within the components also play a role in the formation of the molecular complex. Recently, it was shown that the formation of substituted benzoic acid cocrystals with an acid···acid ring dimer motif was promoted by the presence of electron withdrawing functional group on one benzoic acid and electron donating groups on the other component,[4] using Hammett substituent constants[5] as a quantitative measure of the electron withdrawing and donating nature of the functional groups. Early studies into molecular complexes also noted that for oxygen containing organic species (e.g., aldehydes, ketones, esters, ethers, and carboxylic acids) the stability of molecular complex with an organic acid increased as the strength of the organic acid was increased.[6] This was demonstrated by trichloroacetic acid forming a range of complexes with almost all the substances studied, while monochloroacetic acid and acetic acid only formed a single complex.[7] More recently, work by Aakeröy and co-workers has demonstrated the competition between multiple binding sites within a molecule could be explained by differences in the electrostatic potential of the sites, reflected in the differing pK_as of the functional groups.[8] This highlights that the strength of the intermolecular interactions between the components is dependent on the whole molecular structure. To develop a design strategy based on the effects of electron-withdrawing and -donating groups upon the strength of the supramolecular synthons, a quantitative understanding of these processes is required. The formation of molecular complexes of substituted benzoic acids with benzamide was selected as an initial system for experimental and computational studies into the effects of functional groups upon the formation of a selected supramolecular synthon. The electron-donating and -withdrawing nature of the functional groups on the benzoic acid were varied, the change in binding energy between the components calculated and compared with the success of cocrystallization.

Received: October 20, 2010
Revised: March 3, 2011
Published: March 18, 2011

dx.doi.org/10.1021/cg101403j | *Cryst. Growth Des.* 2011, 11, 1502–1511

Table 1. pK_a Values for Each Selected Coformer, Hammett Constant for the Substituted Benzoic Acids, and Whether or Not They Form Benzamide Molecular Complexes

substance	pK_a	Hammett constant (σ)	forms a Complex?
succinic acid	4.24	N/A	yes
pentafluorobenzoic acid	1.75	0.34 (meta), 0.06 (para)	yes
4-nitrobenzoic acid	3.42	0.71	yes
3-nitrobenzoic acid	3.48	0.78	yes
2-(hydroxymethyl)benzoic acid	3.84	N/A	yes
4-(hydroxymethyl)benzoic acid	4.16	−0.27	yes
picric acid	0.53	N/A	yes
resorcinol	9.45	N/A	yes
salicylic acid	3.01	N/A	yes
benzoic acid	4.20	N/A	no
4-nitrophenol	7.23	N/A	no
5, 5-diallylbarbituric acid	7.80	N/A	no
hexadecanedioic acid	4.48	N/A	no
cinnamic acid	3.88	N/A	no

There have been few previous studies into the formation of benzamide molecular complexes with organic acids. A search of the CSD only returns three complexes; succinic acid (BZASUC),[9] pentafluorobenzoic acid (1:1 ESATUN[10] and 1:2 KEMCEL[11]), whereas the crystal structure of the complex with 4-nitrobenzoic acid has been reported.[12] Additionally, the formation of molecular complexes between benzamide and 2-(hydroxymethyl)benzoic acid, 4-(hydroxymethyl)benzoic acid, 3-nitrobenzoic acid, picric acid, resorcinol (1,3-dihydroxybenzene) and salicylic acid has been identified by hot-stage microscopy but no crystal structures have been determined (during the review of this paper, a crystal structure of the salicylic acid/benzamide was independently determined and published[14]).[13] In contrast, benzoic acid does not form a molecular complex, as indicated by the presence of only a single eutectic point in the binary phase diagram, which has been determined three times independently.[15−17] Four other systems; 5,5-diallylbarbituric acid, 4-nitrophenol, hexadecanedioic acid, and cinnamic acid have also been shown by construction of binary phase diagrams not to form molecular complexes with benzamide.[13] The substituted benzoic acids that form molecular complexes with benzamide all feature electron withdrawing substituents and are stronger acids than benzoic acid (Table 1). In general the stronger acids, as indicated by pK_a values, form molecular complexes, although there are anomalous results, e.g. resorcinol is the weakest acid but forms a complex. This may be due to unsuitability of pK_a values to reflect binding preferences in the solid state or a change in the intermolecular interactions between resorcinol and the other coformers. The resorcinol isomer, quinol (1,4-hydroxybenzene) is well-known host molecule forming numerous inclusion complexes,[18] and although fewer examples are known for resorcinol, it is possible that such a structure is forming in this case, however a clarifying crystal structure determination is still lacking for this system.

Since benzamide has a single amide group capable of participating in hydrogen bonding and the predicted supramolecular synthon for potential cocrystals with benzoic acid is the acid···amide ring dimer (Figure 1). Searching the CSD for the occurrence of this interaction indicates that it is a relatively uncommon supramolecular synthon (Conquest 1.11 on version 5.30 of the CSD,[19] 81 hits, only organics, 3D coordinates

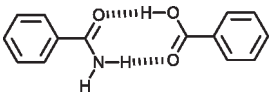

Figure 1. Schematic of acid···amide ring dimer supramolecular synthon.

determined, chemical species >1, a complete list of refcodes is available as Supporting Information). However, because this is the sole hydrogen bonding interaction between these species, it may be possible to predict successful complex formation through the calculation of the energy for this interaction between the components. To test this hypothesis, we determined the interaction for selected substituted benzoic acids by ab initio calculations. The systems selected were the known complex forming acids: pentafluorobenzoic acid (**I**), 4-nitrobenzoic acid (**II**), 3-nitrobenzoic acid (**III**) and salicylic acid (**IV**), the known noncomplexing acids: benzoic acid (**V**), cinnamic acid (**VI**) and acids with unknown complexing ability: 3,5-dinitrobenzoic acid (**VII**), 2,4,6-trihydroxybenzoic acid (**VIII**), 4-aminobenzoic acid (**IX**), 4-hydroxybenzoic acid (**X**), 4-hydroxy 3-nitrobenzoic acid (**XI**), and 4-amino 3-nitrobenzoic acid (**XII**). 3,5-dinitrobenzoic acid and 2,4,6-trihydroxybenzoic acid both contain electron-withdrawing functional groups and are strong acids (pK_a: 2.77, 1.62 respectively) thus they are predicted to form complexes with benzamide. 4-aminobenzoic acid and 4-hydroxybenzoic acid contain electron-donating functional groups and are weaker acids (pK_a: 4.90, 4.57, respectively) and are predicted not to form complexes with benzamide. 4-Hydroxy 3-nitrobenzoic acid and 4-amino 3-nitrobenzoic acid feature a combination of electron-withdrawing and -donating groups and are intermediate in acidity (pK_a: 3.93, 4.19 respectively) but differ in Hammett constant (σ = 0.34, 0.05 respectively). This pair of molecules will test the competition between the additional functional groups. To identify whether a given system forms a molecular complex with benzamide, we undertook synthesis of the molecular complexes by solution and solid-state routes. Where suitable crystals were obtained, crystal structures were determined by single crystal X-ray diffraction. Additionally, the phase diagrams for 4-aminobenzoic acid, 4-hydroxybenzoic acid, 2,4,6-trihydroxybenzoic acid, 4-hydroxy 3-nitrobenzoic acid and 4-amino

Table 2. Experimental Results for the Single-Crystal X-ray Diffraction

system	salicylic acid/ benzamide	3, 5-dinitrobenzoic acid/ benzamide	3-nitrobenzoic acid/ benzamide	4-hydroxy 3-nitrobenzoic acid/benzamide	1, 3, 5-trihydroxybenzene dihydrate
formula	$C_7H_6O_2 \cdot C_7H_7NO_2$	$C_7H_4N_2O_6 \cdot C_7H_7NO_2$	$C_7H_5NO_2 \cdot C_7H_7NO_2$	$C_7H_4NO_5 \cdot C_7H_7NO_2$	$C_6H_6O_3 \cdot 2H_2O$
fw	259.25	333.26	288.26	304.26	162.14
T (K)	100(2)	100(2)	100(2)	100(2)	100(2)
radiation (Å)	Mo K_α, 0.7107	Mo K_α, 0.7107	Mo K_α, 0.7107	Mo K_α, 0.7107	Mo K_α, 0.7107
cryst syst, space group	monoclinic, $P2_1/c$	monoclinic, $P2_1/c$	monoclinic, $P2_1/c$	monoclinic, $P2_1/n$	orthorhombic, *Pnma*
a, b, c (Å)	5.3419(5), 9.5609(8), 23.528(3)	8.4617(18), 10.738(2), 16.049(3)	16.2626(11), 6.8717(4), 11.9800(8)	8.6105(7), 5.0229(3), 30.253(5)	6.5876(5), 13.5170(8), 8.0345(5)
α, β, γ (deg)	90, 91.294(9), 90	90, 99.334(7), 90	90, 107.429(7), 90	90, 98.770(10), 90	90, 90, 90
V (Å^3)	1201.4(2)	1438.9(5)	1277.32(14)	1293.1(3)	715.43
Z, Z', density (g cm^{-3})	4, 1, 1.433	4, 1, 1.538	4, 1, 1.499	4, 1, 1.563	4, 0.5, 1.505
μ (mm^{-1})	0.106	0.126	0.116	0.125	0.133
cryst size (mm)	0.7 × 0.5 × 0.1	0.6 × 0.25 × 0.1	0.5 × 0.1 × 0.07	0.8 × 0.5 × 0.2	1.0 × 0.7 × 0.4
$\theta_{min}/\theta_{max}$	2.75/28.50	2.3/28.1	3.24/28.54	2.93/26.37	2.95/26.37
reflns collected/unique (R_{int})	7148/2714 (0.0564)	8755/3313 (0.033)	7464/2905 (0.0394)	7151/2652 (0.0297)	4322/761 (0.0343)
data/restraints/params	2714/0/174	3313/0/261	2905/0/194	2652/0/199	761/4/71
GOF on F^2	0.936	0.9018	0.945	0.997	0.951
final R indices ($I > 2\sigma(I)$) $R1/wR2$	0.0668/0.1411	0.0384/0.0931	0.0423/0.1015	0.0447/0.0955	0.0463/0.1162
R indices (all data) $R1/wR2$	0.1166/0.1554	0.0529/0.0980	0.0684/0.1095	0.0600/0.0998	0.0598/0.1208
largest diff. peak and hole (e Å^{-3})	0.375/−0.281	0.37/−0.39	0.328/−0.291	0.281/−0.291	0.518/−0.247

3-nitrobenzoic acid with benzamide were investigated through use of the Kofler contact method. In the Kolfer contact method, the highest melting component is initially melted then solidified onto a glass slide. The melted second component is then brought in contact with the first component. This creates a zone of mixing and upon cooling any existing cocrystal phase will form within this region. The resulting mixture exhibits a concentration gradient between each component and so by viewing the heated sample through crossed polar filters, the eutectics between each phase can be identified. If the system exhibits a single eutectic then no cocrystal forms from the melt, while two or more eutectics indicate the formation of a cocrystal phase. This system has been successfully utilized to screen for nicotinamide cocrystals with active pharmaceutical ingredients.[20]

EXPERIMENTAL METHODS

All chemicals were purchased from Sigma-Aldrich in the highest purity available. While the majority of materials have purity greater than 95%, 2,4,6-trihydroxybenzoic acid monohydrate was only available in 90% purity with 1,3,5-trihydroxybenzene as the major impurity. The materials were used as received. The known solubilities of benzamide in methanol and water were used to select initial compositions, with the assumption that the materials would have similar solubilities in these solvents and so production of a congruently dissolving cocrystal will occur at the molar ratio of the cocrystal. A 1:1 composition was selected as the expected composition, although it is noted that variations in cocrystal composition do occur and can be adjusted by solvent choice.[21] Although this does not guarantee the location of all possible cocrystals, this simple solvent screen combined with the hot-stage microscopy and solid-state synthesis should indicate the thermodynamic stability of the system. Metastable cocrystals may occur but location of these would require a significantly more thorough screening process, utilizing crystallization at differing temperatures, controlled cooling and wide range of solvents.

3-Nitrobenzoic acid (1.044 g, 6 mmol) and benzamide (0.7811 g, 6 mmol) were dissolved in methanol (10 mL). Upon slow evaporation, clear needle crystals of the complex were obtained. Salicylic acid (1.139 g, 8 mmol) and benzamide (1.127 g, 9 mmol) were dissolved in water (40 mL). The solution was heated to dissolve the components and then slowly cooled. Clear lustrous plate crystals were obtained. 3, 5-dinitrobenzoic acid (4.0689 g, 19 mmol) and benzamide (2.2836 g, 19 mmol) were dissolved in methanol (25 mL). The solution was heated and stirred to fully dissolve the solid material and left to cool to room temperature. Upon slow evaporation of the solution colorless block crystals were obtained. 2,4,6-trihydroxybenzoic acid monohydrate (0.728 g, 4 mmol) and benzamide (0.6637 g, 5.5 mmol) were dissolved in 95% ethanol (40 mL). Upon slow evaporation light brown block crystals were obtained. 4-hydroxy 3-nitrobenzoic acid (0.8618 g, 5 mmol) and benzamide (0.5648 g, 5 mmol) were dissolved in methanol (15 mL) with gentle heating. Upon cooling yellow plate crystals of the complex were obtained.

Solvent-assisted grinding experiments were carried out for benzamide with 4-aminobenzoic acid (0.2961 g (4aba), 0.3399 g (benzamide)), 4-hydroxybenzoic acid (0.2691 g (4hba), 0.3060 g (benzamide)), 4-amino 3-nitrobenzoic acid (0.3387 g (4a3nba), 0.2312 g (benzamide)) and 2,4,6-trihydroxybenzoic acid (0.3373 g (246thba), 0.2177 g (benzamide)) with 5 drops (approximately 0.5 mL) of 95% ethanol using a ball-mill for 30 min grinding at 30 Hz.

The binary phase diagram between salicylic acid and benzamide was constructed from DSC profiles collected on a TA Q2000 DSC instrument with RGS90 cooling unit. Temperature calibration was performed using an indium metal standard. Mixtures in differing ratios of salicylic acid and benzamide (approximately 5 mg) were weighed directly into Tzero aluminum pans, which were then sealed. The samples were subjected to a heat/cool/heat cycle from 30 to 160 °C with a heating rate of 5°/min. The data from the final run were analyzed using TA Instruments Universal Analysis 2000 software to obtain the solidius and liquidius temperatures from the onset temperature of the eutectic peak and the peak maxima of the higher melting peak.

The solid phases were identified through single crystal and powder X-ray diffraction techniques. A single crystal data set for **VII** was collected at 100 K on a Bruker APEX2 CCD diffractometer equipped with an Oxford Cryosystems low temperature Cryostream device.[22] The data were collected and processed by the APEX2 software. The structure was solved using Sir92[23] and refined using full matrix least-squares on all data using CRYSTALS.[24] All non-hydrogen atoms were anisotropically refined and the hydrogen atoms located in the difference map and freely refined. The structures of **III**, **IV**, **VIII**, and **XI** were determined by single crystal diffraction at 100 K on an Oxford X-caliber2 diffractometer with Mo K_α radiation with a graphite monochromator using an Oxford

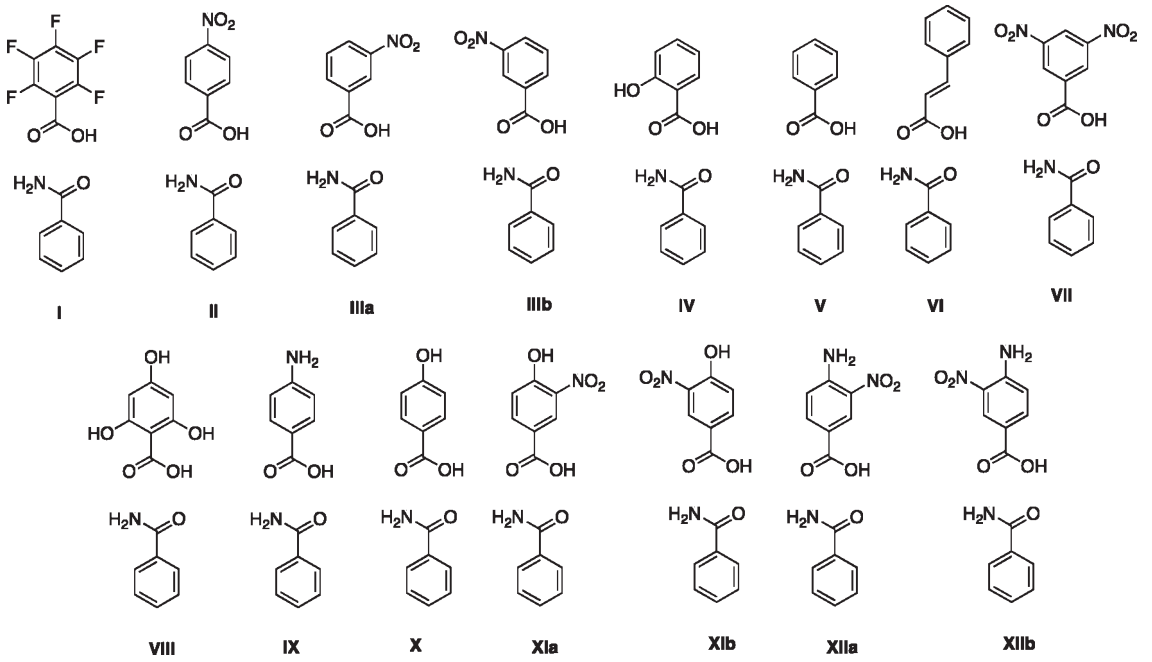

Figure 2. Molecular structures of benzamide dimers with pentafluorobenzoic acid (**I**), 4-nitrobenzoic acid (**II**), 3-nitrobenzoic acid (two conformations **IIIa, IIIb**), salicylic acid (**IV**), benzoic acid (**V**), cinnamic acid (**VI**), 3, 5-dinitrobenzoic acid (**VII**), 2, 4, 6-trihydroxybenzoic acid (**VIII**), 4-aminobenzoic acid (**IX**), 4-hydroxybenzoic acid (**X**), 4-hydroxy 3-nitrobenzoic acid (two conformations **XIa, XIb**), and 4-amino 3-nitrobenzoic acid (two conformations **XIIa, XIIb**).

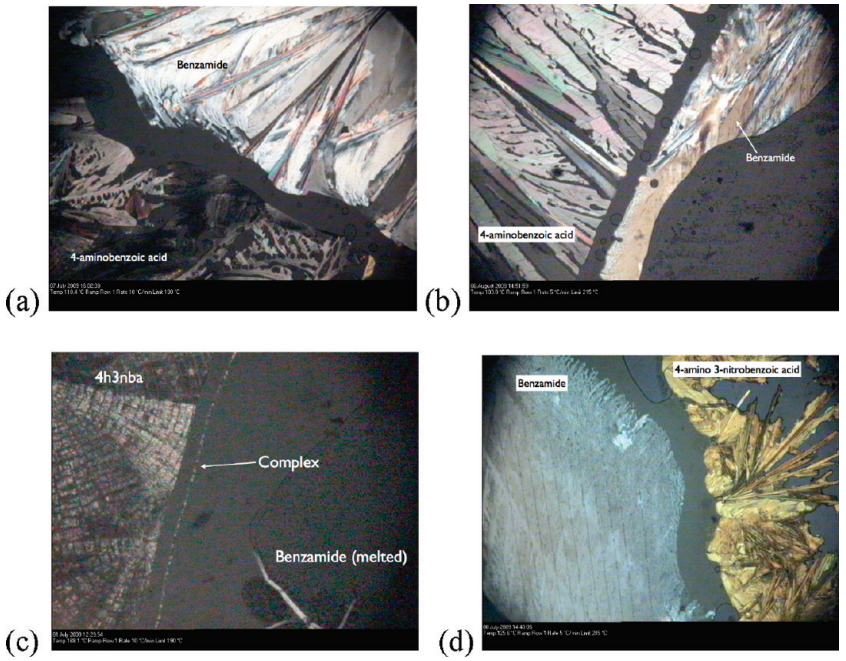

Figure 3. Kolfer Contact Images for the systems (a) **IX**, (b) **X**, (c) **XI**, and (d) **XII**.

Cryosystems Cryostream 700 to maintain the temperature. The data were collected and processed using CryAlisPro software.[25] Structure solution was carried out using Shelxs97[26] and the structured refined against F^2 for all reflections by full matrix methods in Shelxl97.[26] All non-hydrogen atoms were refined anisotropically and the hydrogen atoms were placed in geometric positions and refined as riding atoms except for those bound to oxygen and nitrogen, which were freely refined. Single crystal studies into the crystals obtained from 2,4,6-trihydroxybenzoic acid and benzamide identified them as the dihydrate of 1,3,5-trihydroxybenzene. The previously published structure[27] was used as an initial model for the structure refinement. The hydrogen atoms that are lacking in the previous study were located from the Fourier difference map and refined using AFIX 147 (hydroxybenzene hydrogens) and DFIX (water hydrogens) constraints. The hydrogen atom temperature factors were constrained by the values of the bonding atoms. Details of the final refinements are given in Table 2.[28]

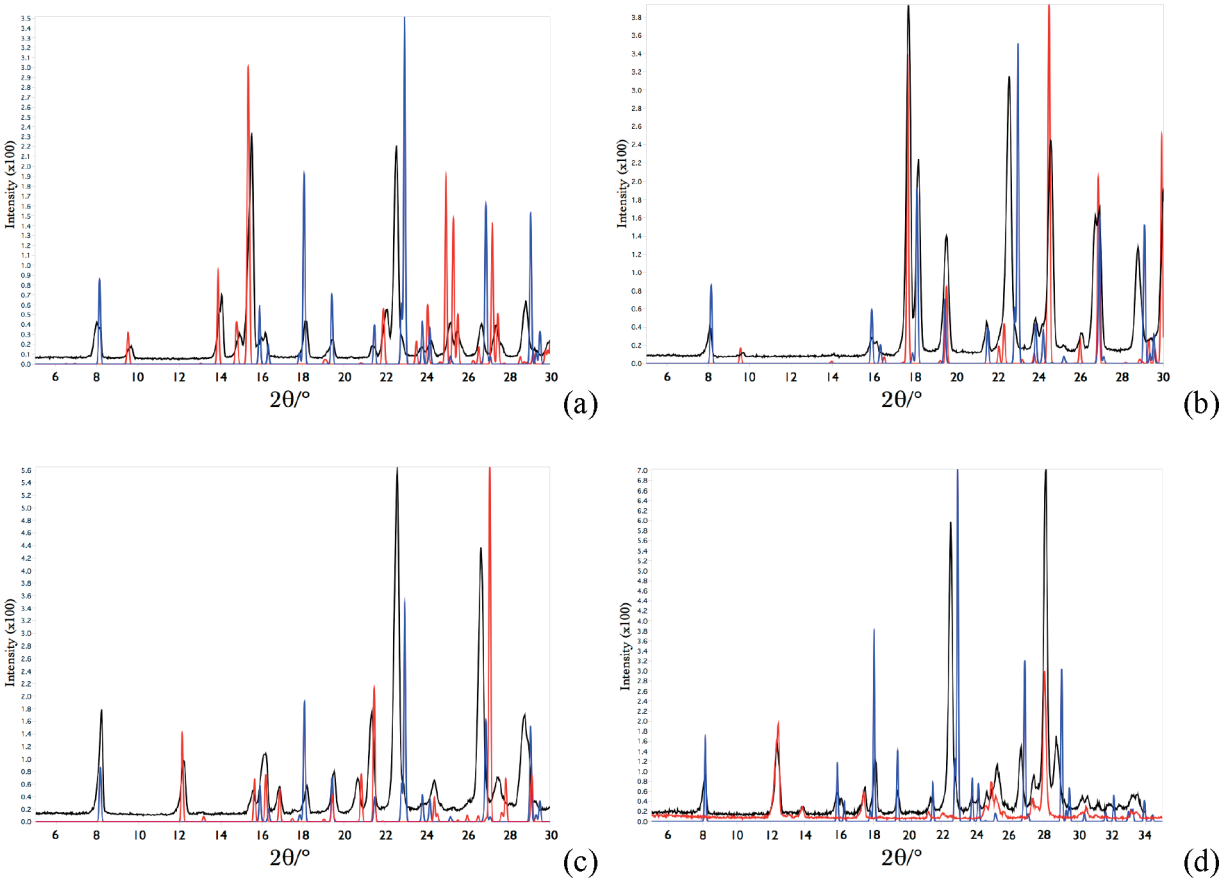

Figure 4. PXRD of product from ethanol assisted grinding of benzamide with (a) 4-aminobenzoic acid, (b) 4-hydroxybenzoic acid, (c) 4-amino 3-nitrobenzoic acid, and (d) 2,4,6-trihydroxybenzoic acid. The experimental results are shown in black, a simulated pattern of benzamide in blue, and the substituted benzoic acid in red.

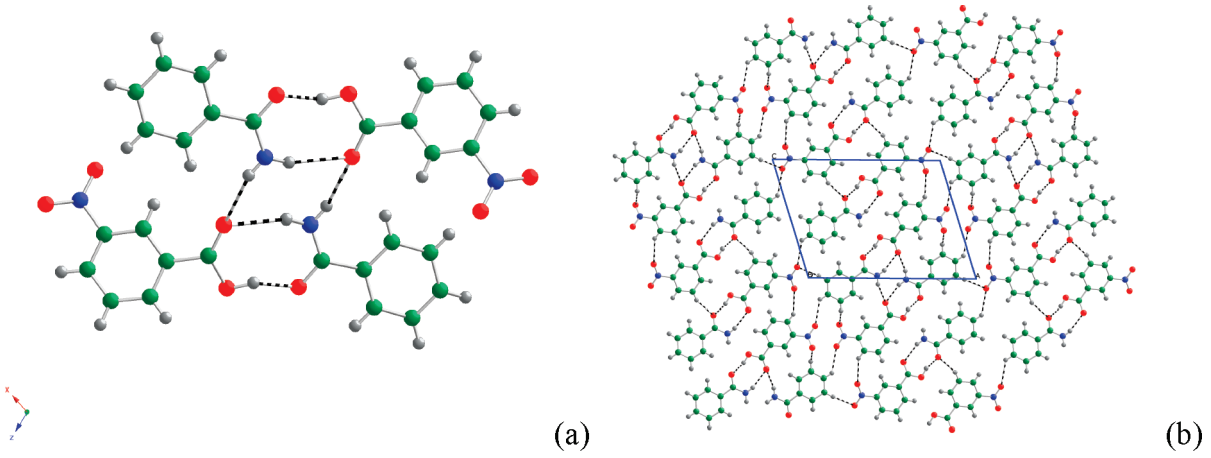

Figure 5. (a) Formation of tetramer structure in **III** by a combination of strong hydrogen bonds. (b) Packing of dimers into a 2D sheet structure. Carbon atoms are shown as green spheres, oxygen atoms as red, nitrogen atoms as blue, and hydrogen atoms as gray.

COMPUTATIONAL METHODS

The intermolecular energy calculations were carried out using the program orca[29] with the initial molecular dimer constructed in Avogadro. The initial model was optimized at the PBE/VDZ(P) level and then the energies calculated at PBE/TVZP with the TVZ/J auxiliary basis set using the Ahlrichs basis sets[30] and polarization.[31] The Ahlrichs auxiliary basis sets were obtained from the TurboMole basis set library under ftp.chemie.unikarlsruhe.de/pub/jbasen.[32] These are valence triple-ζ basis sets with a polarization contribution and offer a suitable level of theory to evaluate these weak interactions. After optimization and evaluation of the dimer and individual monomers, the basis set superposition error was evaluated by applying the counterpoise method.[33] The final intermolecular energy was then calculated using eq 1, where E_{inter} is the intermolecular energy, E^{opt} is the energy of the optimized structure, E^{AB} is the

dx.doi.org/10.1021/cg101403j |*Cryst. Growth Des.* 2011, 11, 1502–1511

energy of A and B in the geometry of the dimer and E^{counter} is the energy of A or B in the dimer with "ghost" atoms at the other molecule sites.

$$E_{\text{inter}} = E_{\text{AB}}^{\text{opt}} - E_{\text{A}}^{\text{opt}} + E_{\text{B}}^{\text{opt}}(E_{A}^{\text{AB}} - E_{\text{A}}^{\text{counter}} = E_{\text{B}}^{\text{AB}} - E_{\text{B}}^{\text{counter}}) \quad (1)$$

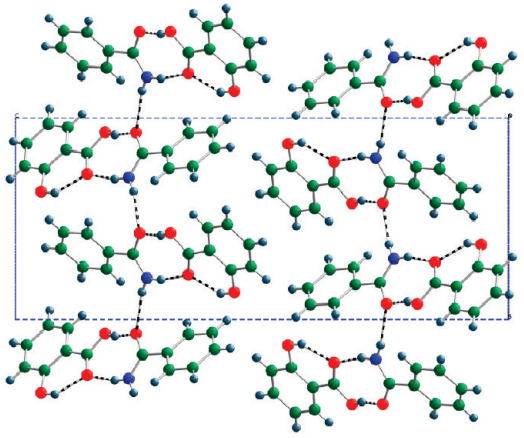

Figure 6. View along the *a*-axis of **IV**, showing the formation of molecular ribbons between the salicylic acid:benzamide dimer, which then pack together to form the 3D structure. The atom colors are the same as in Figure 4.

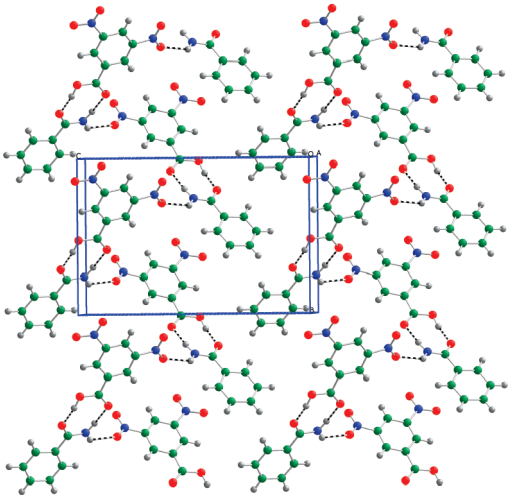

Figure 7. Formation of molecular ribbon in the crystal structure of **VII**, with the interactions between the ribbons forming the 2D ladder. The atom colors are the same as in Figure 4.

In the cases of 3-nitrobenzoic acid, 4-hydroxy 3-nitrobenzoic acid, and 4-amino 3-nitrobenzoic acid, two different conformations were considered because they are systems that are not symmetric relative to the carboxylic acid functional group (Figure 2).

The lattice energy for the salicylic acid/benzamide cocrystal and series of potential benzoic acid/benzamide cocrystals was evaluated using the Dreiding force field[34] and Gasteiger atomic point charges[35] in the Material Studio program.[36] Hypothetical benzoic acid/benzamide cocrystals were constructed from the existing crystal structures by replacing the substituent groups with hydrogens, followed by energy minimization of the cell parameters and atom positions. The salicylic acid/benzamide cocrystal structure and the crystal structures of the single component phases were also fully optimized using the same method. The optimized energy includes contributions from both conformational and intermolecular interaction terms and so the lattice energy of each system was calculated using eq 2, where E_{latt} is the lattice energy, E_{crystal}, the calculated energy of crystal, N_i, the number of molecules of type i, E^i_{conf}, the conformational energy of molecule of type i and n, the number of different molecules.

$$E_{\text{lattice}} = \frac{E_{\text{crystal}}}{\sum_{i=0}^{n} N_i} - \sum_{i=0}^{n} E^i_{\text{conf}} \quad (2)$$

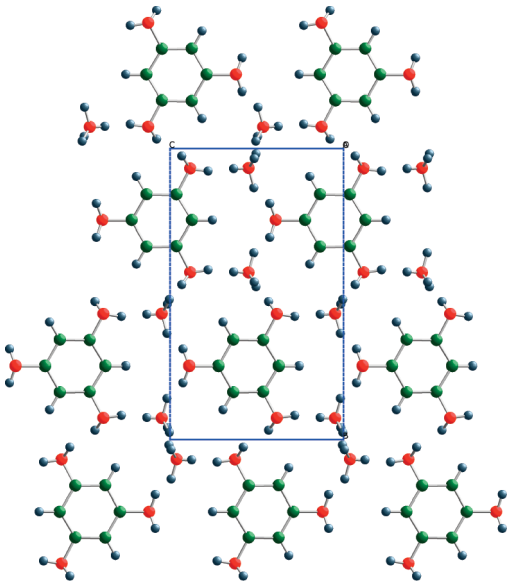

Figure 9. Formation of 2D sheet in the structure of trihydroxybenzene dihydrate, by disordered orientations of water and O−H groups, viewed down the *a*-axis.

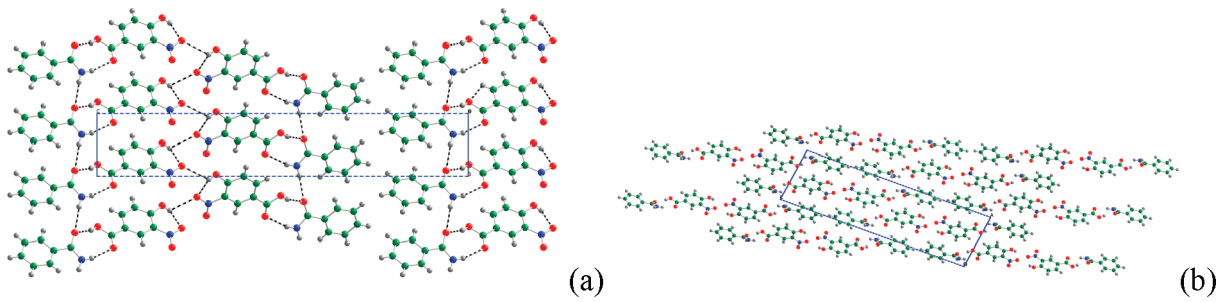

Figure 8. (a) Formation of a 1D ribbon between the dimer units of **XI**, then packing into a sheet structure through O−H···O_{nitro} and C−H···π interactions. (b) Packing of the sheets into the final 3D structure.

dx.doi.org/10.1021/cg101403j |*Cryst. Growth Des.* 2011, 11, 1502–1511

Table 3. Geometric Parameters for the Acid···Amide $R^2_2(8)$ Dimer Motif in the Benzamide Cocrystals

syst	$d_{C=Oacid}$ (Å)	d_{C-OH} (Å)	$d_{C=Oamide}$ (Å)	d_{C-NH2} (Å)	$d_{O\cdots N}$ (Å)	$d_{O\cdots O}$ (Å)
III	1.212(2)	1.319(2)	1.239(2)	1.331(2)	3.042(1)	2.525(1)
IV	1.228(3)	1.323(3)	1.248(3)	1.327(3)	2.926(3)	2.602(2)
VII	1.228(2)	1.329(2)	1.261(2)	1.346(2)	2.933(2)	2.589(2)
XI	1.214(2)	1.324(2)	1.253(2)	1.325(2)	3.048(2)	2.559(2)

Table 4. Energy of Hydrogen-Bonding Interaction for Each Species with Benzamide[a]

substance	energy (kJ mol^{-1})
benzamide	−54.183
cinnamic acid	−61.452
4-aminobenzoic acid	−62.255
4-hydroxybenzoic acid	−62.380
benzoic acid	−63.511
salicylic acid	−63.556
4-amino 3-nitrobenzoic acid	−64.8267/−65.7539
pentafluorobenzoic acid	−67.492
4-nitrobenzoic acid	−67.897
4-hydroxy 3-nitrobenzoic acid	−68.268/−67.159
3-nitrobenzoic acid	−68.513/−68.589
2, 4, 6-trihydroxybenzoic acid	−71.495
3, 5-dinitrobenzoic acid	−72.501

[a] The values for 3-nitrobenzoic acid, 4-hydroxy 3-nitrobenzoic acid and 4-amino 3-nitrobenzoic acid are given for the two conformations of the nitro group.

RESULTS

Hot-Stage Microscopy and Solvent-Assisted Grinding. The application of the Kolfer contact method to **IX**, **X**, and **XII** indicated that no cocrystal was stable by the presence of a single eutectic (Figure 3a, b, d). This was supported by solution crystallization and solvent-assisted grinding experiments that produced mixtures of the starting materials (Figure 4a−c). For **XI**, a clear single 1:1 cocrystal phase is observed in the experiment (Figure 3c), which has a melting point intermediate to the starting materials (169 °C versus 126 and 190 °C, respectively). For **VIII**, the hot-stage experiment was unable to be performed due to the thermal degradation of the trihydroxybenzoic acid upon heating, whereas the PXRD of the solvent-assisted grinding experiment appears to suggest that cocrystallization has not occurred as the majority of peaks match the starting materials (Figure 4d). However, there are weak peaks at higher angle that may be due to a new phase and so the results of the study into **VIII** are inconclusive.

Crystal Structure Analysis. III forms a 1:1 complex where the dimer is formed through an acid...amide interaction between the O−H···O and N−H···O interactions, forming a second level $R^2_2(8)$ motif. The nitro groups packs on the amide side of benzamide forming motif **IIIb**. Pairs of dimers are held together by a discrete N−H···O=C_{acid} interaction (Figure 5a). These pairs of dimers pack into 1D ladders along the *a*-axis through weaker C−H···O=C_{amide} and C−H···O_{nitro} interactions. Further C−H···O_{nitro} interactions form 2D sheets from these ladders (Figure 5b), which then pack through $\pi\cdots\pi$ interactions along the *b*-axis to form the final 3D structure.

IV also forms a 1:1 molecular complex. The ortho-hydroxy group in salicylic acid forms an intramolecular O−H···O hydrogen bond with the carboxylic acid group. The dimer is formed through an acid···amide interaction between the O−H···O and N−H···O interactions, forming a second level $R^2_2(8)$ motif. These dimers then bind through a C(5) N−H···O hydrogen bond between the benzamide amide groups to form a ribbon along the *b*-axis (Figure 6). These ribbons are stacked along the *a*-axis through $\pi\cdots\pi$ interactions, while C−H···π interactions between the ribbons complete the 3D crystal structure (Figure 6).

VII is a 1:1 molecular complex with the dimer bound together through the expected acid···amide interaction by an O−H···O and N−H···O hydrogen bonds that combine together to form a second level $R^2_2(8)$ motif. These dimers form a discrete N−H···O_{nitro} hydrogen bond and in combination with the acid...amide interaction a ribbon (second level $C^4_4(20)$ motif) is formed along the *b*-axis around the 2_1 screw axis (Figure 7). These stacks are interwoven with each other and held together by $\pi\cdots\pi$ interactions to form a 2D ladder structure (Figure 7). The ladders are packed together to form the final 3D structure through C_{aryl}−H···O_{nitro} hydrogen bonds.

XI forms a 1:1 molecular complex with the dimer again formed through the O−H···O/N−H···O acid/amide $R^2_2(8)$ hydrogen bonds. Again, the nitro group is on the same side of dimer as the amide NH_2 group forming motif **XIb**. These dimers form a 1D ribbon along the *b*-axis through a N−H···O_{amide} C(4) hydrogen bond (Figure 8a). These ribbons pack into a 2D sheet lying in the *bc*-plane through an O−H···O_{nitro} hydrogen bond. This hydrogen is bifurcated between this interaction and an intramolecular interaction with the ortho nitro group (Figure 8b). The combination of these two interactions form a second level C(3) motif. The final 3D structure is generated through the packing of the sheets by $\pi\cdots\pi$ interactions.

The dihydrate of 1,3,5-trihydroxybenzene forms a layered structure, through OH...O hydrogen bonds between hydroxybenzene and the water molecules (Figure 9). The hydroxyl groups display an orientational proton disorder due to the symmetry of crystal as the mirror plane of the unit cell lines through the middle of the hydroxybenzene molecule. The remaining OH group of the water links the sheets into the final 3D crystal structure through a OH···O hydrogen bond to a water molecule in the plane above.

Intermolecular Interactions. There is little variation in the geometry of the acid···amide interaction between the various complexes (Table 3). The systems that successfully form cocrystals only introduce additional hydrogen bond acceptor sites as the two hydroxyl containing systems (**IV** and **XI**) form intramolecular hydrogen bonds. These additional binding sites, however, generally do not compete as the other acceptor sites in amide and acid motifs. Although all form the same acid···amide interaction to bind the two components together, the second hydrogen of the benzamide is involved in a variety of NH···O hydrogen

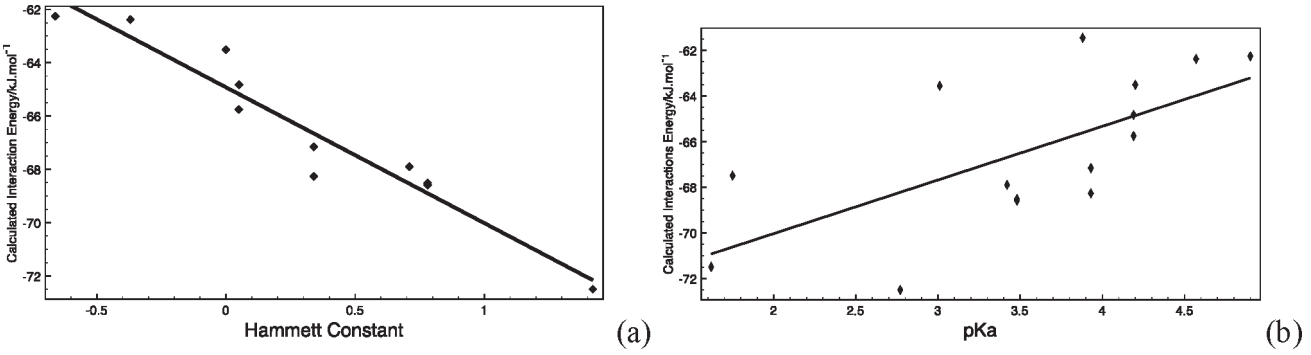

Figure 10. (a) Plot of calculated hydrogen-bonding energy against the Hammett constants for each benzoic acid, (b) plot of calculated hydrogen-bonding energies against the pK_a values for each benzoic acid. In each case, a linear correlation line has been fitted by least-squares ((a) R^2 = 0.982, (b) R^2 = 0.436).

Table 5. Calculated Crystal Energies, Lattice Energies, and Shifts in Unit-Cell Parameters of Known Salicyclic Acid/Benzamide Cocrystal, Hypothetical Benzoic Acid/Benzamide Co-Crystal, and Individual Components

system	calcd cryst energy (kJ mol^{-1})	lattice energy (kJ·mol^{-1})	shift in unit-cell params *a*, *b*, *c*, β (Å, deg)	energy of cocrystal formation (kJ mol^{-1})[a]
salicylic acid/benzamide	−226.13	−159.57	−0.5342, 0.4418, 0.0005, −2.607	+29.18
benzoic acid/benzamide (from SA/BZA)	−175.27	−154.33	−0.5234, 0.3965, −0.3781, −2.589	+22.53
benzoic acid/benzamide (from 3,5-DNBA/BZA)	−126.06	−147.84	0.1779, −0.0261, 1.8771, 16.455	+29.02
benzoic acid/benzamide (from 4H3NBA/BZA)	−175.21	−155.62	−2.1458, −0.0954, 4.8415, −19.319	+21.24
benzoic acid/benzamide (from 3-NBA/BZA)	−156.04	−153.84	1.0868, −0.0146, −0.8768, −0.967	+23.02
salicylic acid	−117.69	−90.86	−1.6663, 2.2751, 0.1605, 11.103	N/A
benzamide	−110.43	−97.89	0.2615, −0.0669, −1.6526, 2.08	N/A
benzoic acid	−51.26	−78.97	0.4508, −0.2717, −1.2162, −4.49	N/A

[a] $E_{formation} = E^{AB}{}_{latt} - (E^{A}{}_{latt} + E^{B}{}_{latt})$.

bonds. In **III**, the carbonyl group of the acid is utilized in an intramolecular interaction with the OH group and so is unavailable to form intermolecular interactions with the amide group, thus the NH···O_{amide} is the only remaining interaction available to construct the crystal lattice. For the remaining systems, all three feature the same 3-nitrobenozic acid fragment with differing substituents. In **IV**, a NH···O═C_{acid} hydrogen bond is formed and the nitro group is only involved in weaker CH···O bonding. In **XI**, an intramolecular interaction occurs between the OH and nitro groups further reducing the effectiveness of the nitro group as an acceptor. The additional electron donating contribution of the OH group may also reduce the effectiveness of the carbonyl oxygen of the acid group as a hydrogen donor as the NH···O_{acid} interaction observed in **IV** is replaced by an NH···O_{amide} interaction. In **VII**, the additional group is an electron withdrawing nitro group, which appears to improve the hydrogen-bond-accepting capabilities of the neighboring nitro as the NH···O_{acid} interaction in **IV** is replaced by a NH···O_{nitro} interaction. Thus the interactions between the various functional groups plays an important role in both controlling the formation of the dimer between the component and the subsequent growth of the crystal structure.

Binding Energies. The calculated energies from the ab initio calculations are presented in Table 4. For comparison, the hydrogen-bonding energy between two benzamide molecules was also calculated, which shows that the interaction between the acid and amide is a stronger interaction the amide···amide interaction. Previous studies into the calculation of dimer interactions between acid and amide groups show the same conculsion.[37] The ordering of the acid···acid interactions, in general, agrees with the experimental results, with the strongest interactions belonging to those pairs that successfully form complexes except for **VIII** where the experimental evidence for cocrystallization is inconclusive. Plotting the predicted hydrogen bonding energy against the value of the Hammett constant for the various complexes displays a linear correlation between the two parameters (Figure 10a). In contrast, plotting the energy against the pK_a values (Figure 10b) for the acids shows a weaker correlation. Thus the Hammett constant appears to be a stronger predictor for complex formation in this case than pK_a. However, the lack of Hammett constants for ortho positions highlights the limitations of this approach. In addition, the prediction of the molecular conformation displayed by the meta-substituted systems is inconclusive. Although the lowest energy conformation for **III** is the conformation observed in the crystal structure, this is not the case for **XI**, where the higher energy conformation is observed. However, given the important role played by all intermolecular interactions in controlling the final crystal packing, this may not be unexpected.

The difference in binding energy for benzoic acid and salicylic acid is insignificant (<0.05 kJ mol^{-1}), yet one system forms a cocrystal, whereas the other does not. This further indicates that the interaction between the acid and amide groups alone does not control the overall formation of the crystalline complex. To investigate the role the other packing forces may be playing in the selectivity of cocrystal formation, we evaluated the lattice energy for the salicylic acid/benzamide and series of hypothetical benzoic acid/benzamide cocrystals (Table 5). The calculated energy of the salicylic acid/benzamide cocrystal is lower than all

Table 6. Intermolecular Interaction Energies (sum of 200 interactions) around Each Component in the Hypothetical Benzoic Acid/Benzamide Cocrystals, Salicylic Acid/Benzamide, and the Single-Component Crystal Structures

system	cluster energy (kJ mol^{-1}) (benzamide, benzoic acid)
salicylic acid/benzamide	−103.32, −96.06
benzoic acid/benzamide (from SA/BZA)	−101.98, −87.62
benzoic acid/benzamide (from 3,5-DNBA/BZA)	−78.33, −73.46
benzoic acid/benzamide (from 4H3NBA/BZA)	−92.34, −84.11
benzoic acid/benzamide (from 3-NBA/BZA)	−92.08, −83.94
salicylic acid	−99.81
benzamide	−98.61
benzoic acid	−84.32

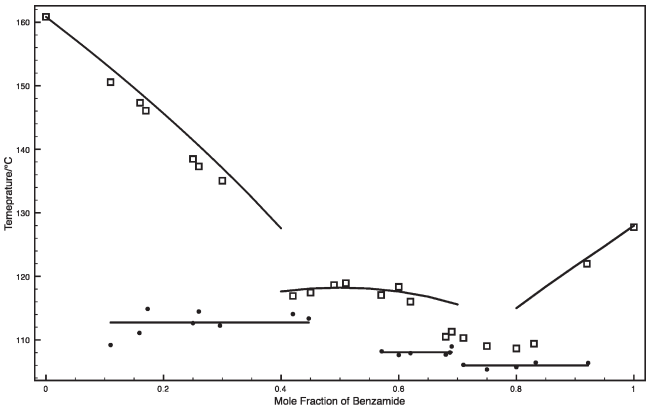

Figure 11. Constructed binary phase diagram for salicylic acid and benzamide. Experimental liquidius points are shown as open squares, experimental solidius points as shown as filled circles, and calculated ideal curves as black lines.

the potential benzoic acid/benzamide systems generated and so the additional interactions within the structure may be favoring the formation of the cocrystal in the salicylic acid case. To further investigate the differences between the two structures, we evaluated the bonding environment in Mercury (version 2.4)[38] with the intermolecular interactions evaluated using the UNI forcefield.[39] The geometry of the benzamide molecule undergoes little to no change between the five optimized structures with only the torsion angle of the amide group relative to the benzene ring changing in the range 150−170°. The energy of molecular clusters around each component in each structure and the single component phases was evaluated (Table 6), which shows that the stronger intermolecular interactions are experienced by both molecules in the salicylic acid/benzamide cocrystal compared to the potential benzoic acid systems. However, the calculation of the energy of the cocrystal formation for the systems indicates that all are unfavored compared to individual components (Table 5). This may be due to the simplistic model used for the energy calculations, although previous computational studies into the prediction of cocrystals formation,[40] also failed to predict the formation of the succinic acid/benzamide system compared to the stable polymorph of benzamide. This failure was suggested to be due to the sensitivity of the force fields used to the pyramidalization of the benzamide amide group. However, the enthalpy of formation of a cocrystal may be determined experimentally from the heat of fusion of the cocrystal and starting components and consideration of the binary phase diagram.[41] A number of multicomponent systems have shown to be entropically stabilized and have a positive enthalpy of formation.[42] The binary phase diagram (Figure 11) for salicylic acid/benzamide indicates that the cocrystal has a lower melting point than either of the two starting materials. Such a phase diagram for racemic compounds is taken as evidence for weak binding between the enatiomers[43] and so by comparison it would be expected that the cocrystal to have a low energy of formation. The enthalpy of formation determined from the phase diagram is 24.71 kJ mol^{-1} and so the cocrystal phase must be entropically stabilized. This highlights a potential limitation of the application of computational methods to cocrystal screening.

CONCLUSIONS

Although a cocrystal between benzamide and benzoic acid is thermodynamically unfeasible, cocrystal phases can be created through the addition of electron withdrawing groups to the benzoic acid (positive Hammett constants). Ab initio DFT calculations indicate that one contribution to the improved stability is the increased strength of the intermolecular acid···amide interaction between the two components, which correlates with the sign of the Hammett constant. However, this alone is not enough to successfully predict the formation of a new cocrystal, as shown by salicylic acid and 2,4,6-trihydroxybenzoic acid. Although the salicylic acid/benzamide system has a similar binding energy as the benzoic acid/benzamide system but does successfully form a cocrystal, the 2,4,6-trihydroxybenzoic acid/benzamide has one of the strongest binding energies but conclusive evidence of cocrystallization was not obtained. Comparison of the lattice energies for salicylic acid/benzamide and hypothetical benzoic acid/benzamide crystal structures generated from the other known cocrystals indicates that potential benzoic acid/benzamide cocrystals are less stable by up to 10 kJ mol^{-1} compared to the known cocrystals and so the other packing forces play an important role in the successful formation of cocrystal phase. However, calculation of the energy of cocrystal formation for all cases indicates that the cocrystal is unstable relative to the separate phases. Experimental determination of the binary phase diagram for the salicylic acid/benzamide system reveals that the cocrystal has a lower melting point than both single components and a positive enthalpy of formation indicates that the cocrystal is entropically stabilized. Thus the development of predictive tools for cocrystallization requires the continued experimental and computational investigations into both successful and unsuccessful cocrystallization to gain insight into the factors that influence and control the cocrystallization process.

ASSOCIATED CONTENT

Supporting Information. Crystallographic information for each of the single crystal structure determinations (as .cif and corresponding .fcf). Refcode list of structures displaying the acid···amide ring dimer (as .pdf). This material is available free of charge via the Internet at http://pubs.acs.org.

AUTHOR INFORMATION

Corresponding Author

*E-mail: Colin.Seaton@manchester.ac.uk. Tel: +44 (0)161 3064362.

■ ACKNOWLEDGMENT

We thank Prof. Roger J. Davey and Dr Ghasala Sadiq for fruitful discussions on the applications of Hammett substitution constants to cocrystallisation and Bradford University for access to the DSC equipment to collect the binary phase diagram.

■ REFERENCES

(1) Etter, M. C. *Acc. Chem. Res.* **1990**, *23* (4), 120. Burchell, C. J.; Ferguson, G.; Lough, A. J.; Glidewell, C. *Acta Crystallogr., Sect. B* **2000**, *56*, 1054. Bond, A. D. *Chem. Commun.* **2003**, 250. Aakeröy, C. B.; Salmon, D. J. *CrystEngComm* **2005**, *7*, 439. Arora, K. K.; PrakashaReddy, J.; Pedireddi, V. R. *Tetrahedron* **2005**, *61*, 10792. Balevicius, V.; Barisevicute, R.; Bernstein, J. *Chem. Commun.* **2005**, 5007. Bhogala, B. R.; Basavju, S.; Nangia, A. *CrystEngComm* **2005**, *7*, 551. Aidas, K.; Svoboda, I.; Ehrenberg, H.; Fuess, H. *Phys. Chem. Chem. Phys.* **2007**, *9*, 3181. Bis, J. A.; Vishweshwar, P.; Weyna, D.; Zaworotko, M. J. *Mol. Pharm.* **2007**, *4*, 401. Chadwick, K.; Davey, R. J.; Cross, W. I. *CrystEngComm* **2007**, *9*, 732. Chiarella, R. A.; Davey, R. J.; Peterson, M. L. *Cryst. Growth Des.* **2007**, *7*, 1223. Parkin, A.; Seaton, C. C.; Blagden, N.; Wilson, C. C. *Cryst. Growth Des.* **2007**, *7*, 531. Bhogala, B. R.; Nangia, A. *New J. Chem.* **2008**, *32*, 800. Braga, D.; Palladino, G.; Polito, M.; Rubini, K.; Grepioni, F.; Chierotti, M. R.; Gobetto, R. *Chem.—Eur. J.* **2008**, *14* (32), 10149. Cincic, D.; Friscic, T.; Jones, W. *Chem.—Eur. J.* **2008**, *14*, 747. Polito, M.; D'oria, E.; Maini, L.; Karamertzanis, P. G.; Grepioni, F.; Braga, D.; Price, S. L. *CrystEngComm* **2008**, *10* (12), 1848. Karki, S.; Friscic, T.; Jones, W. *CrystEngComm* **2009**, *11* (3), 470. Martins, D. M. S.; Middlemiss, D. S.; Pulham, C. R.; Wilson, C. C.; Weller, M. T.; Henry, P. F.; Shankland, N.; Shankland, K.; Marshall, W. G.; Ibberson, R. M.; Knight, K.; Moggach, S.; Brunelli, M.; Morrison, C. A. *J. Am. Chem. Soc.* **2009**, *131* (11), 3884. Skovsgaard, S.; Bond, A. D. *CrystEngComm* **2009**, *11* (3), 444. Corvis, Y.; Négrier, P.; Lazerges, M.; Massip, S.; Léger, J.-M.; Espeau, P. *J. Phys. Chem B.* **2010**, *114*, 5420. Thorey, P.; Bombicz, P.; Szilagyi, I. M.; Molnar, P.; Bansaghi, G.; Szekely, E.; Simandi, B.; Parkanyi, L.; Pokol, G.; Madarasz, J. *Thermochim. Acta* **2010**, *497* (1−2), 129.

(2) Almarsson, O.; Zaworotko, M. J. *Chem. Commun.* **2004**, 1889. Stahly, G. P. *Cryst. Growth Des.* **2007**, *7*, 1007. Caira, M. R. *Mol. Pharmaceutics* **2007**, *4*, 310. Shand, N.; Zaworotko, M. J. *Drug Discovery Today* **2008**, *13* (9/10), 440. Miroshnyk, I.; Mirza, S.; Sandlert, N. *Expert Opin. Drug Del.* **2009**, *6* (4), 333. Schartman, R. R. *Int. J. Pharm.* **2009**, *365* (1−2), 77.

(3) Desiraju, G. R. *Angew. Chem., Int. Ed.* **1995**, *34* (21), 2311.

(4) Chadwick, K.; Sadiq, G.; Davey, R. J.; Seaton, C. C.; Pritchard, R. G.; Parkin, A. *Cryst. Growth Des.* **2009**, *9* (3), 1278. Seaton, C. C.; Chadwick, K.; Sadiq, G.; Guo, K.; Davey, R. J. *Cryst. Growth Des* **2010**, *10* (2), 726.

(5) Hansch, C.; Leo, A.; Taft, R. W. *Chem. Rev.* **1991**, *91* (2), 165.

(6) Kendall, J.; Booge, J. E.; Andrews, J. C. *J. Am. Chem. Soc.* **1918**, *40*, 2303.

(7) Kendall, J. *J. Am. Chem. Soc.* **1914**, *36*, 1222. Kendall, J. *J. Am. Chem. Soc.* **1914**, *36*, 1722. Kendall, J.; Gibbons, W. A. *J. Am. Chem. Soc.* **1915**, *37*, 149. Kendall, J. *J. Am. Chem. Soc.* **1916**, *38*, 1309. Kendall, J.; Booge, J. E. *J. Am. Chem. Soc.* **1916**, *38*, 1712.

(8) Aakeröy, C. B.; Salmon, D. J.; Smith, M. M.; Desper, J. *Cryst. Growth Des.* **2006**, *6* (4), 1033. Aakeröy, C. B.; Salmon, D. J.; Smith, M. M.; Desper, J. *CrystEngComm.* **2009**, *11*, 439. Aakeröy, C. B.; Rajbanshi, A.; Li, Z. J.; Desper, J. *CrystEngComm.* **2010**, *12* (12), 4231.

(9) Huang, C.-M.; Leiserowitz, L.; Schmidt, G. M. J. *J. Chem. Soc., Perkin Trans. 2* **1973**, 503.

(10) Reddy, L. S.; Nangia, A.; Lynch, V. M. *Cryst. Growth Des.* **2004**, *4* (1), 89.

(11) Jankowski, W.; Gdaniec, M.; Polonski, T. *Acta Crystallogr., Sect. C* **2006**, *62*, o492.

(12) Blagden, N.; Berry, D. J.; Parkin, A.; Javed, H.; Ibrahim, A.; Gavan, P. T.; De Matos, L. L.; Seaton, C. C. *New J. Chem.* **2008**, *32* (10), 1659.

(13) Quehenberger, H. *Monatsh. Chem.* **1949**, 595.

(14) Elbagerma, M. A.; Edwards, H. G. M.; Munshi, T.; Scowen, I. J. *Anal. Bioanal. Chem.* **2010**, *397* (1), 137.

(15) Sharma, B. L.; Sharma, N. K.; Bassi, P. S. *Cryst. Res. Technol.* **1982**, *17* (9), 1117.

(16) Brittain, H. G. *Cryst. Growth Des.* **2009**, *9* (5), 2492.

(17) Singh, N. B.; Das, S. S.; Singh, N. P.; Agrawal, T. *J. Cryst. Growth* **2008**, *310* (11), 2878.

(18) Herbstein, F. H *Crystalline Molecular Complexes and Compounds*; Oxford University Press: Oxford, U.K., 2005.

(19) Bruno, I. J.; Cole, J. C.; Edgington, P. R.; Kessler, M.; Macrae, C. F.; McCabe, P.; Pearson, J.; Taylor, R. *Acta Crystallogr., Sect B* **2002**, *58*, 389.

(20) Berry, D. J.; Seaton, C. C.; Clegg, W.; Harrington, R. W.; Coles, S. J.; Horton, P. N.; Hursthouse, M. B.; Storey, R.; Jones, W.; Friscic, T.; Blagden, N. *Cryst. Growth Des.* **2008**, *8* (5), 1697.

(21) Seaton, C. C.; Parkin, A.; Wilson, C. C.; Blagden, N. *Cryst. Growth Des.* **2009**, *9* (1), 47. Jayasankar, A.; Reddy, L. S.; Bethune, S. J.; Rodriguez-Hornedo, N. *Cryst. Growth Des.* **2009**, *9* (2), 889. Boyd, S.; Back, K.; Chadwick, K.; Davey, R. J.; Seaton, C. C. *J. Pharm. Sci.* **2010**, *99* (9), 3779.

(22) *APEX2: Area-Detector Software Package*; Bruker Nonius: Madison, WI, 2006.

(23) Altomare, A.; Cascarano, G.; Giacovazzo, G.; Guagliardi, A.; Burla, M. C.; Polidori, G.; Camalli, M. *J. Appl. Crystallogr.* **1994**, *27*, 435.

(24) Betteridge, P. W.; Carruthers, J. R.; Cooper, R. I.; Prout, K.; Watkin, D. J. *J. Appl. Crystallogr.* **2003**, *36*, 1487.

(25) *CrysAlisPro*, Oxford Diffraction Ltd, Abingdon, UK, 2009.

(26) Sheldrick, G. M. *Acta Crystallogr., Sect. A* **2008**, *64*, 112.

(27) Wallwork, S. C.; Powell, H. M. *Acta Crystallogr.* **1957**, *10* (1), 48.

(28) CCDC 797156−797160 contain the supplementary crystallographic data for this paper. These data can be obtained free of charge from The Cambridge Crystallographic Data Centre via www.ccdc.cam.ac.uk/data_request/cif.

(29) Neese, F. *ORCA, an Ab Initio, Density Functional and Semi-Empirical Program Package*; University of Bonn: Bonn, Germany, 2008; http://www.thch.uni-bonn.de/tc/orca.

(30) Schaefer, A.; Horn, H.; Ahlrichs, R. *J. Chem. Phys.* **1992**, *97*, 2571.

(31) Ahlrichs, R. and coworkers, unpublished.

(32) Eichkorn, K.; Treutler, O.; Ohm, H.; Haser, M.; Ahlrichs, R. *Chem. Phys. Lett.* **1995**, *240*, 283. Eichkorn, K.; Weigend, F.; Treutler, O.; Ahlrichs, R. *Theor. Chem. Acc.* **1997**, *97*, 119.

(33) Boys, S. F.; Bernardi, F. *Mol. Phys.* **1970**, *19* (4), 553.

(34) Mayo, S. L.; Olafson, B. D.; Goddard, W. A. *J. Phys. Chem.* **1990**, *94*, 8897.

(35) Gasteiger, J.; Marsili, M. *Tetrahedron* **1980**, *36*, 3219.

(36) *Materials Studio Version 4.0*; Accerlys Software Inc.: San Diego, CA.

(37) Vishweshwar, P.; Nangia, A.; Lynch, V. M. *Cryst. Growth Des.* **2003**, *3* (5), 783.

(38) Macrae, C. F.; Bruno, I. J.; Chisholm, J. A.; Edgington, P. R.; McCabe, P.; Pidcock, E.; Rodriguez-Monge, L.; Taylor, R.; van de Streek, J.; Wood, P. A. *J. Appl. Crystallogr.* **2008**, *41*, 466.

(39) Gavezzotti, A. *Acc. Chem. Res.* **1994**, *27*, 309–314. Gavezzotti, A.; Filippini, G. *J. Phys. Chem.* **1994**, *98* (18), 4831.

(40) Issa, N.; Karamertzanis, P. G.; Welch, G. W. A.; Price, S. L. *Cryst. Growth Des.* **2009**, *9* (1), 442.

(41) Beoerio-Goates, J.; Goates, S. R.; Ott, J. B.; Goates, J. R. *J. Chem. Thermodyn.* **1985**, *17* (7), 665.

(42) Abdel-Rehiem, A. G.; Farrell, P. G.; Westwood, J. V. *J. Chem. Soc., Faraday Trans. 1* **1975**, *71*, 1762. Goates, S. R.; Boerio-Goates, J.; Goates, J. R.; Ott, J. B. *J. Chem. Soc., Faraday Trans. 1* **1987**, *83* (5), 1553–1558. Ott, J. B.; Goates, J. R. *J. Chem. Eng. Data* **1996**, *41* (4), 669.

(43) Jaques, J.; Collet, A.; Wilen, S. H. *Enantiomers, Racemates and Resolutions*; Krieger: Malabar, 1994.